

Efficient numerical schemes for the solution of generalized time fractional Burgers type equations

Zohreh Asgari¹ · S. M. Hosseini¹

Received: 30 July 2016 / Accepted: 3 May 2017 / Published online: 13 May 2017
© Springer Science+Business Media New York 2017

Abstract The main aim of this paper is to propose two semi-implicit Fourier pseudospectral schemes for the solution of generalized time fractional Burgers type equations, with an analysis of consistency, stability, and convergence. Under some assumptions, the unconditional stability of the schemes is shown. In implementation of these schemes, the fast Fourier transform (FFT) can be used efficiently to improve the computational cost. Various test problems are included to illustrate the results that we have obtained regarding the proposed schemes. The results of numerical experiments are compared with analytical solutions and other existing methods in the literature to show the efficiency of proposed schemes in both accuracy and CPU time. As numerical solution of fractional stochastic nonlinear partial differential equations driven by Brownian motions are among current related research interests, we report the performance of these schemes on stochastic time fractional Burgers equation as well.

Keywords Stochastic time fractional Burgers equation · Fourier pseudospectral · Consistency · Stability · Convergence · Additive noise

✉ Zohreh Asgari
z.asgari@modares.ac.ir

S. M. Hosseini
hossei_m@modares.ac.ir

¹ Department of Applied Mathematics, Tarbiat Modares University, P.O.Box 14115-175, Tehran, Iran

1 Introduction

In this paper, we study the generalized time fractional Burgers type equations

$${}_a^c D_t^\alpha u(x, t) + (u)^p u_x - \beta u_{xx} + \gamma u_{xxxx} = f(x, t), \quad (x, t) \in \Omega, \quad (1.1)$$

where $\Omega = \{(x, t) | x_L < x < x_R, 0 < t \leq T\}$, $p > 0$, $\beta > 0$, $\gamma \geq 0$, $0 < \alpha < 1$, the boundary conditions are periodic as $u(x_L, t) = u(x_R, t)$, initial condition is denoted by u_0 , $f(x, t)$ is a given function, and ${}_a^c D_t^\alpha$ is the Caputo fractional partial derivative of order α and is defined as follows

$${}_0^c D_t^\alpha u(x, t) = \frac{1}{\Gamma(1-\alpha)} \int_0^t \frac{\partial u(x, s)}{\partial s} \frac{ds}{(t-s)^\alpha}, \quad \alpha \in (0, 1), \quad (1.2)$$

in which $\Gamma(\cdot)$ denotes the gamma function. For $p = 1$ and $\gamma = 0$, (1.1) is actually the time fractional Kuramoto-Sivashinsky (KS) equation, and for $p = 1$ and $\gamma = 0$ it reduces to time fractional Burgers equation.

The fractional Burgers equation is used to describe the physical processes of uni-directional propagation of weakly nonlinear acoustic waves through a gas-filled pipe [25]. The fractional derivative results from the cumulative effect of the wall friction through the boundary layer. The same form can also be found in other models such as shallow-water waves and waves in bubbly liquids [25, 35, 36]. Moreover, the KS equation appears in context of long waves on the interface between two viscous fluids, unstable drift waves in plasmas, and flame front instability [24]. This model is a common nonlinear evolution equation arising in a variety of physical contexts, e.g., long waves on thin films, reaction diffusion systems, etc..

In the literature, there are some numerical and semi-analytical methods for the solution of nonlinear time fractional Burgers and KS equations. Authors of [33] constructed the analytical solutions of the fractional KS equation by a new proposed method via fractional complex transform. The cubic parametric spline functions was developed for obtaining an approximate solution for the time fractional Burgers equation in [10]. This equation has been solved by Adomian decomposition method in [18], Lie group method in [16], variational iteration method in [39], and homotopy analysis method in [7, 34]. The solutions obtained by the above methods were calculated in a form of convergent series. Authors of [23] compared the results of generalized transformation technique and homotopy perturbation method for the numerical solution of time fractional Burgers equation. A spectral shifted Legendre collocation method for both temporal and spatial discretizations of space-time fractional Burgers equation is given in [3]. Based on the improved generalized exp-function method, the space-time fractional Burgers and Sharma-Tasso-Olver equations were studied in [1] and the authors discussed the single-wave, double-wave, three-wave, and four-wave solutions. Haar wavelet scheme and optimal homotopy asymptotic

method are presented in [17]. The moving boundary space-time fractional Burger's equation is studied in [2] using the fractional Riccati expansion method. Time fractional diffusion equation and time fractional Burgers-Fisher equation are solved in [13] with Haar wavelet method where fractional derivatives are Caputo derivative. The quadratic B-spline Galerkin method and finite element method based on the cubic B-spline collocation approach without any analysis have also been given in [11, 12] for the time fractional Burgers equation. A linear implicit finite difference scheme for solving the fractional Burgers equation has been proposed in [25]; their proposed finite difference method is unconditionally stable and convergent of order $\mathcal{O}(\tau + h^2)$.

In this paper, we propose two semi-implicit Fourier pseudospectral schemes of orders $\mathcal{O}(\tau + h^m)$ and $\mathcal{O}(\tau^{2-\alpha} + h^m)$ for the solution of time fractional generalized Burgers equation (1.1). Obviously, order of convergence in one of the proposed schemes here changes with fractional order α and improves with $\alpha \rightarrow 0^+$. We discretize the spatial terms using a Fourier collocation (pseudospectral) method, and the fractional time derivative is then approximated with an implicit procedure. Then, the consistency, stability, and convergence of the proposed schemes are discussed. The order of convergence and the unconditional stability of the schemes, under some assumptions, are obtained. During the computation, we use the fast Fourier transform to improve the computational cost. We compare the results of our proposed schemes with the results of [25] in terms of accuracy and CPU time and show the efficiency and capability of proposed methods. We also examine the efficiency of proposed schemes for the solution of system of time fractional PDEs with considering stochastic time fractional Burgers equation with additive noise.

As many readers know, spectral and pseudospectral methods have been developed for numerical simulation of related differential equations in many fields because of its high accuracy, especially in sufficiently smooth problems. Obviously, Fourier collocation method is a natural choice to obtain the optimal spatial accuracy when we have the periodic boundary condition. There is a wide and varied literature on the spectral schemes and there has been a significant growth in these fields in the past two decades, especially for time-dependent nonlinear PDEs. For instance, the analysis of method for 1D conservation laws is given by Tadmor in [31, 32], semi-discrete viscous Burgers' equation and Navier-Stokes equations by E [9], Fourier spectral projection method for Navier-Stokes equations by Guo and Zou [15], and a fully discrete pseudospectral method for the viscous Burgers, Boussinesq and regularized long wave equations, by [6, 14, 22].

This article is outlined as follows. In Section 2, we first review the Fourier spectral and pseudospectral differentiations and then we introduce our two numerical schemes for the time fractional equation (1.1). In Section 3, the consistency analysis of the schemes are studied. The stability and convergence analysis of schemes are given in Sections 4 and 5. In Section 6, the results of numerical experiments are compared with available analytical solutions and results of a recently reported method. We further illustrate numerically the impact of fractional order α and other parameters on the theoretical features of the schemes already obtained in previous sections.

2 Some introductory results and the proposed new numerical schemes

Before proposing our numerical schemes, we give here some formulas and properties of the pseudospectral approximation. Let $f(x) \in L^2(\Omega)$, $\Omega = (0, a)$, with Fourier series

$$f(x) = \sum_{l=-\infty}^{\infty} \hat{f}_l e^{2\pi ilx/a}, \quad \hat{f}_l = \frac{1}{a} \int_{\Omega} f(x) e^{-2\pi ilx/a} dx. \tag{2.1}$$

The truncated series which is defined as the projection of $f(x)$ onto the \mathcal{B}^N , the space of trigonometric polynomials in x of degree up to N , is given by

$$\mathcal{P}_N f(x) = \sum_{l=-N}^N \hat{f}_l e^{2\pi ilx/a}. \tag{2.2}$$

However, to obtain a pseudospectral approximation of the above function at a given set of points, an interpolation operator \mathcal{I}_N is introduced. The Fourier interpolation of a given function f on the uniform numerical grid with $(2N + 1)$ points is given as

$$(\mathcal{I}_N f)(x) = \sum_{l=-N}^N (\hat{f}^N)_l e^{2\pi ilx/a}. \tag{2.3}$$

The pseudospectral coefficients $(\hat{f}^N)_l$ are computed by imposing interpolation conditions at mentioned equidistant points. Note that to obtain $(\mathcal{I}_N f)(x)$, we only need the values of $f(x)$ at a set of suitable grid points. So, for given $\Omega, h = \frac{a}{2N+1}$ (the step size of spatial variable), $x_j = jh, j = 0, 1, \dots, 2N$, and $f_j = f(x_j)$, considering \mathbf{f} as the discrete vector function containing grid values $f(x_j)$, we will use $(\mathcal{I}_N f)$ and $(\mathcal{I}_N \mathbf{f})$ with the same meaning as (2.3). If $f(x)$ and all its derivatives up to m th order are continuous and periodic then the convergence of the derivatives of the projection and interpolation is given by [5]

$$\begin{aligned} \left\| \partial^k f(x) - \partial^k \mathcal{P}_N f(x) \right\|_{L^2} &\leq \left\| f^{(m)} \right\|_{L^2} h^{m-k}, & \text{for } 0 \leq k \leq m, \\ \left\| \partial^k f(x) - \partial^k \mathcal{I}_N f(x) \right\|_{L^2} &\leq \|f\|_{H^m} h^{m-k}, & \text{for } 0 \leq k \leq m, m > \frac{1}{2}, \end{aligned} \tag{2.4}$$

and

$$\|f\|_{L^2} = \left(\int_{\Omega} f^2(x) dx \right)^{1/2}, \quad \|f\|_{H^m} = \left(\int_{\Omega} \sum_{|n| \leq m} |(D^n f(x))^2| dx \right)^{1/2}.$$

For any collocation approximation to the function $f(x)$ at the interpolation point x_j

$$f_j = (\mathcal{I}_N f)_j = \sum_{l=-N}^N (\hat{f}^N)_l e^{2\pi ilx_j/a}, \tag{2.5}$$

we can also define discrete differentiation operator \mathcal{D}_N operating on the vector grid function \mathbf{f} . In application, one may compute the collocation coefficients $(\hat{f}^N)_l$ via

FFT, and then multiply them by the true values (given by $\frac{2\pi il}{a}$) and perform the inverse FFT. Alternatively, we can view the differentiation operator \mathcal{D}_N as matrix, and the above process can be seen as a matrix-vector multiplication [14]. In fact, for the second and fourth derivatives $\partial_x^2, \partial_x^4$, the differentiation matrix can be applied for multiple times, that is, the vector \mathbf{f} is multiplied by \mathcal{D}_N^2 and \mathcal{D}_N^4 respectively.

For periodic vector grid functions \mathbf{f} and \mathbf{g} , we define the l^2 inner product and norm as

$$\|\mathbf{f}\|_2 = \sqrt{\langle \mathbf{f}, \mathbf{f} \rangle}, \quad \text{with} \quad \langle \mathbf{f}, \mathbf{g} \rangle = h \sum_{j=0}^{2N} \mathbf{f}_j \mathbf{g}_j. \tag{2.6}$$

Hence, we can write [14]

$$\langle \mathbf{f}, D_N \mathbf{g} \rangle = - \langle D_N \mathbf{f}, \mathbf{g} \rangle, \quad \langle \mathbf{f}, D_N^2 \mathbf{g} \rangle = - \langle D_N \mathbf{f}, D_N \mathbf{g} \rangle, \quad \langle \mathbf{f}, D_N^4 \mathbf{g} \rangle = \langle D_N^2 \mathbf{f}, D_N^2 \mathbf{g} \rangle. \tag{2.7}$$

For positive integer number M , let $\tau = \frac{T}{M}$ be the time step size, i.e., we have

$$t_n = n\tau, \quad n = 0, 1, \dots, M.$$

For discretization of time fractional derivative we use the following L1 scheme which is studied in [8, 19, 20, 26, 37].

Lemma 2.1 *Suppose $0 < \alpha < 1$ and $g(t) \in C^2[0, t_n]$, then*

$$\left| \frac{1}{\Gamma(1-\alpha)} \int_0^{t_n} \frac{g'(t)}{(t_n-t)^\alpha} dt - \frac{\tau^{-\alpha}}{\Gamma(2-\alpha)} \left[a_0 g(t_n) - \sum_{k=1}^{n-1} (a_{n-k-1} - a_{n-k}) g(t_k) - a_{n-1} g(t_0) \right] \right| \leq \frac{1}{\Gamma(2-\alpha)} \left[\frac{1-\alpha}{12} + \frac{2^{2-\alpha}}{2-\alpha} - (1+2^{-\alpha}) \right] \max_{0 \leq t \leq t_n} |g''(t)| \tau^{2-\alpha},$$

where $a_k = (k+1)^{1-\alpha} - k^{1-\alpha}$.

The following lemmas are then needed in analyzing our proposed numerical schemes.

Lemma 2.2 [37]. *If $0 < \alpha < 1$ and $a_k = (k+1)^{1-\alpha} - k^{1-\alpha}$, $k = 0, 1, \dots$, then*

$$1 = a_0 > a_1 > \dots > a_k \rightarrow 0, \quad \text{as } k \rightarrow \infty.$$

Lemma 2.3 *Similar to [14] it can be shown that for any $f \in \mathcal{B}^{pN}$ (with p an integer) we have*

$$\|\mathcal{I}_N f\|_{H^k} \leq \sqrt{p} \|f\|_{H^k}, \quad \text{for any integer } k \geq 0.$$

Lemma 2.4 (discrete Gronwall’s inequality [30]) *Assume that $\{q_n\}$ and $\{p_n\}$ are nonnegative sequences and the sequence $\{\phi_n\}$ satisfies*

$$\phi_0 \leq g_0, \quad \phi_n \leq g_0 + \sum_{k=0}^{n-1} p_k + \sum_{k=0}^{n-1} q_k \phi_k, \quad n \geq 1,$$

where $g_0 \geq 0$. Then the sequence $\{\phi_n\}$ satisfies

$$\phi_n \leq \left(g_0 + \sum_{k=0}^{n-1} p_k \right) \exp \left(\sum_{k=0}^{n-1} q_k \right), \quad n \geq 1.$$

Lemma 2.5 Using Taylor series expansion for $u(x, t)$, we have

- a) $\partial_x \left(u^{p+1} \right) \Big|_{(x, t_{n-1})} = \partial_x \left(u^{p+1} \right) \Big|_{(x, t_n)} - \tau \partial_{tx} \left(u^{p+1} \right) \Big|_{(x, t_n)} + \mathcal{O}(\tau^2),$
- b) $\partial_x \left(u^{p+1} \right) \Big|_{(x, t_{n-\frac{1}{2}})} = \frac{3}{2} \partial_x \left(u^{p+1} \right) \Big|_{(x, t_{n-1})} - \frac{1}{2} \partial_x \left(u^{p+1} \right) \Big|_{(x, t_{n-2})} + \mathcal{O}(\tau^2).$
- c) $u(x, t_{n-\frac{1}{2}}) = \frac{1}{2} (u(x, t_n) + u(x, t_{n-1})) + \mathcal{O}(\tau^2),$
- d) $u(x, t_{n-\frac{1}{2}}) = \frac{3}{4} u(x, t_n) + \frac{1}{4} u(x, t_{n-2}) + \mathcal{O}(\tau^2).$

2.1 The new schemes

Now, we propose two semi-implicit Fourier pseudospectral schemes for the solution of time fractional PDE (1.1).

Scheme I:

We first discretize the time fractional derivative using the scheme described in Lemma 2.1 which is of order $\mathcal{O}(\tau^{2-\alpha})$. Let $u^k := u(x, t_k)$ and \mathbf{u}^k be the numerical vector solution which is evaluated at discrete grid points and in time level k . To approximate nonlinear term, we can use the first order method presented in [25] which is as follows

$$u^p \frac{\partial u}{\partial x} \Big|_{(x, t_n)} \simeq \frac{1}{p+2} \left[(u^{n-1})^p u_x^n + \left((u^{n-1})^p u^n \right)_x \right]. \tag{2.8}$$

Let u^n be unknown, then for calculating the Fourier transform of right-hand side of (2.8), one needs to evaluate convolution of two functions which is expensive. Hence, we approximate the nonlinear term, using Lemma 2.5 (a), i.e., as

$$\partial_x \left(u^{p+1} \right) \Big|_{(x, t_n)} \simeq \partial_x \left(u^{p+1} \right) \Big|_{(x, t_{n-1})},$$

and propose the following scheme,

$$\mu \left[a_0 \mathbf{u}^n - \sum_{k=1}^{n-1} (a_{n-k-1} - a_{n-k}) \mathbf{u}^k - a_{n-1} \mathbf{u}^0 \right] - \beta \mathcal{D}_N^2 \mathbf{u}^n + \gamma \mathcal{D}_N^4 \mathbf{u}^n + \frac{1}{p+1} \mathcal{D}_N \left(\mathbf{u}^{n-1} \right)^{p+1} = \mathbf{f}^n, \tag{2.9}$$

where $\mu = \frac{\tau^{-\alpha}}{\Gamma(2-\alpha)}$ and \mathbf{f}^n is the vector values of $f(x, t)$ at discrete grid points and time level t_n . We will show that Scheme I is convergent of order $\mathcal{O}(\tau + h^m)$.

Scheme II:

In scheme I, although the order of time derivative is $\mathcal{O}(\tau^{2-\alpha})$ but this order can be seriously affected by the approximating order of nonlinear term. Hence, to avoid this effect and improve the order of scheme in the time-dependent part of equation, we use Lemma 2.5 (b)-(d) and propose the following scheme,

$$\begin{aligned} & \mu \left[a_0 \left(\frac{\mathbf{u}^n + \mathbf{u}^{n-1}}{2} \right) - \sum_{k=1}^{n-1} (a_{n-k-1} - a_{n-k}) \left(\frac{\mathbf{u}^k + \mathbf{u}^{k-1}}{2} \right) - a_{n-1} \mathbf{u}^0 \right] \\ & - \beta \mathcal{D}_N^2 \left(\frac{3}{4} \mathbf{u}^n + \frac{1}{4} \mathbf{u}^{n-2} \right) \\ & + \gamma \mathcal{D}_N^4 \left(\frac{3}{4} \mathbf{u}^n + \frac{1}{4} \mathbf{u}^{n-2} \right) + \frac{1}{p+1} \mathcal{D}_N \left(\frac{3}{2} (\mathbf{u}^{n-1})^{p+1} - \frac{1}{2} (\mathbf{u}^{n-2})^{p+1} \right) \\ & = \left(\frac{3}{4} \mathbf{f}^n + \frac{1}{4} \mathbf{f}^{n-2} \right). \end{aligned} \tag{2.10}$$

We will show that the Scheme II is convergent of order $\mathcal{O}(\tau^{2-\alpha} + h^m)$.

Remark 2.1 Since scheme II is a three-step method, we first use the Scheme I at first level to obtain \mathbf{u}^1 and then employ the Scheme II.

3 Consistency analysis

In this section, by similar idea as in [14, 22], we will analyze the consistency of proposed schemes for the solution of fractional equation (1.1). In the consistency analysis, instead of a direct comparison between the numerical solution and the exact solution, we construct an approximate solution by projecting the exact solution in the spatial variable onto \mathcal{B}^N [14]. The consistency analysis shows that in Scheme I, such an approximate solution satisfies the numerical scheme up to an $\mathcal{O}(\tau)$ accuracy in time and a spectral accuracy in space. We first recall some space functions and norms which will be used in our analysis as follows:

$$\begin{aligned} \|f\|_{L^2(0,T;H^r)} &= \left(\int_0^T \|f\|_{H^r}^2 dt \right)^{\frac{1}{2}}, \quad \|f\|_{L^\infty(0,T;H^r)} = \sup_{0 \leq t \leq T} \|f\|_{H^r}, \\ \|f\|_{l^2(0,T;H^r)} &= \sqrt{\tau \sum_{k=0}^M \|f^k\|_{H^r}^2}, \quad \|f\|_{l^\infty(0,T;H^r)} = \max_{0 \leq k \leq M} \|f^k\|_{H^r}, \quad M = \left\lceil \frac{T}{\tau} \right\rceil. \end{aligned}$$

3.1 Analysis of truncation error for U_N

Let $u_e(x, t)$ be the exact solution of (1.1) and, in view of (2.2), define $F_N(x, t) = \mathcal{P}_N f(x, t)$,

$$U_N(x, t) = \mathcal{P}_N u_e(x, t).$$

From (2.4), we have

$$\|U_N - u_e\|_{L^\infty(0,T;H^r)} \leq Ch^m \|u_e\|_{L^\infty(0,T;H^{m+r})}, \quad r \geq 0, \tag{3.1}$$

$$\|F_N - f\|_{L^\infty(0,T;L^2)} \leq Ch^m \|f\|_{L^\infty(0,T;H^m)}, \tag{3.2}$$

$$\left\| \partial_x^2 (U_N - u_e) \right\|_{L^2} \leq Ch^m \|u_e\|_{H^{m+2}}, \tag{3.3}$$

$$\left\| \partial_x^4 (U_N - u_e) \right\|_{L^2} \leq Ch^m \|u_e\|_{H^{m+4}}, \tag{3.4}$$

where C is a constant which has different values in different occurrences. As

$${}^c D_t^\alpha U_N(x, t) = {}^c D_t^\alpha \mathcal{P}_N u_e(x, t) = \mathcal{P}_N {}^c D_t^\alpha u_e(x, t),$$

we can write

$$\left\| {}^c D_t^\alpha (U_N - u_e) \right\|_{L^2} \leq Ch^m \left\| {}^c D_t^\alpha u_e \right\|_{H^m}. \tag{3.5}$$

Now, we rewrite the above relations in the discrete norm $\|\cdot\|_2$ which has been used in the truncation error derivation. Since $\partial_x^2 U_N \in \mathcal{B}^N$, so $\mathcal{I}_N \partial_x^2 U_N = \partial_x^2 U_N$, and we have

$$\left\| \partial_x^2 \mathbf{U}_N - \partial_x^2 \mathbf{u}_e \right\|_2 = \left\| \mathcal{I}_N \left(\partial_x^2 (U_N - u_e) \right) \right\|_{L^2} \leq \left\| \partial_x^2 (U_N - u_e) \right\|_{L^2} + \left\| \mathcal{I}_N \partial_x^2 u_e - \partial_x^2 u_e \right\|_{L^2}, \tag{3.6}$$

where $\partial_x^2 \mathbf{U}_N$ and $\partial_x^2 \mathbf{u}_e$ are vector grid functions of $\partial_x^2 U_N$ and $\partial_x^2 u_e$ respectively. The second term of (3.6) could be bounded by

$$\left\| \mathcal{I}_N \left(\partial_x^2 u_e \right) - \partial_x^2 u_e \right\|_{L^2} \leq Ch^m \left\| \partial_x^2 u_e \right\|_{H^m} \leq Ch^m \|u_e\|_{H^{m+2}}. \tag{3.7}$$

Then, from (3.3) and (3.7), we have

$$\left\| \partial_x^2 \mathbf{U}_N - \partial_x^2 \mathbf{u}_e \right\|_2 \leq Ch^m \|u_e\|_{H^{m+2}}. \tag{3.8}$$

In a similar manner, we can write

$$\left\| \partial_x^4 \mathbf{U}_N - \partial_x^4 \mathbf{u}_e \right\|_2 \leq Ch^m \|u_e\|_{H^{m+4}}, \tag{3.9}$$

$$\left\| {}^c D_t^\alpha \mathbf{U}_N - {}^c D_t^\alpha \mathbf{u}_e \right\|_2 \leq Ch^m \left\| {}^c D_t^\alpha u_e \right\|_{H^m}. \tag{3.10}$$

For the nonlinear term, we can write [22]

$$\begin{aligned} (u_e)^p (u_e)_x - (U_N)^p (U_N)_x &= (U_N)^p (u_e - U_N)_x + [(u_e)^p - (U_N)^p] (u_e)_x \\ &= (U_N)^p (u_e - U_N)_x \\ &\quad + (u_e)_x (u_e - U_N) \sum_{k=0}^{p-1} (u_e)^k (U_N)^{p-1-k}. \end{aligned} \tag{3.11}$$

Using the Young and Hölder inequalities

$$\begin{aligned} \|(U_N)^p(u_e - U_N)\|_{L^2} &\leq \|(U_N)^p\|_{L^\infty} \|u_e - U_N\|_{L^2}, \\ \|(u_e)^k (U_N)^{p-1-k}\|_{L^\infty} &= \left\| (u_e)^{(p-1)\frac{k}{p-1}} (U_N)^{(p-1)(1-\frac{k}{p-1})} \right\|_{L^\infty} \\ &\leq \frac{k}{p-1} \|(u_e)^{p-1}\|_{L^\infty} + \left(1 - \frac{k}{p-1}\right) \|(U_N)^{p-1}\|_{L^\infty}, \end{aligned}$$

and also 1D Sobolev embedding and (3.11), we obtain

$$\begin{aligned} \|(u_e)^p(u_e)_x - (U_N)^p(U_N)_x\|_{L^2} &\leq C \left(\|(U_N)^p\|_{L^\infty} \|u_e - U_N\|_{H^1} + \|u_e - U_N\|_{L^\infty} \right. \\ &\quad \left. \times \left[\|u_e\|_{L^\infty}^{p-1} + \|U_N\|_{L^\infty}^{p-1} \right] \|u_e\|_{H^1} \right) \\ &\leq C \|u_e - U_N\|_{H^1} \|u_e\|_{H^1}^p \leq Ch^m \|u_e\|_{H^{m+1}} \|u_e\|_{H^1}^p. \end{aligned} \tag{3.12}$$

Hence, we get

$$\begin{aligned} \|(\mathbf{u}_e)^p(\mathbf{u}_e)_x - (\mathbf{U}_N)^p(\mathbf{U}_N)_x\|_2 &= \frac{1}{p+1} \left\| \partial_x (\mathbf{u}_e)^{p+1} - \partial_x (\mathbf{U}_N)^{p+1} \right\|_2 \\ &= \frac{1}{p+1} \left\| \mathcal{I}_N \left(\partial_x \left[(u_e)^{p+1} - (U_N)^{p+1} \right] \right) \right\|_{L^2} \\ &= \frac{1}{p+1} \left\| \partial_x \left[(u_e)^{p+1} - (U_N)^{p+1} \right] - \partial_x (u_e)^{p+1} \right. \\ &\quad \left. + \mathcal{I}_N \partial_x (u_e)^{p+1} + \partial_x (U_N)^{p+1} - \mathcal{I}_N \partial_x (U_N)^{p+1} \right\|_{L^2} \\ &\leq \frac{1}{p+1} \left(\left\| \partial_x \left[(u_e)^{p+1} - (U_N)^{p+1} \right] \right\|_{L^2} \right. \\ &\quad \left. + \left\| \partial_x (u_e)^{p+1} - \mathcal{I}_N \partial_x (u_e)^{p+1} \right\|_{L^2} \right. \\ &\quad \left. + \left\| \partial_x (U_N)^{p+1} - \mathcal{I}_N \partial_x (U_N)^{p+1} \right\|_{L^2} \right) \\ &\leq Ch^m \|u_e\|_{H^1}^p \|u_e\|_{H^{m+1}}. \end{aligned} \tag{3.13}$$

Note that, in (3.13), we used the following relations

$$\begin{aligned} \left\| \partial_x (u_e)^{p+1} - \mathcal{I}_N \partial_x (u_e)^{p+1} \right\|_{L^2} &\leq Ch^m \left\| \partial_x (u_e)^{p+1} \right\|_{H^m} \leq Ch^m \|u_e\|_{H^1}^p \|u_e\|_{H^{m+1}}, \\ \left\| \partial_x (U_N)^{p+1} - \mathcal{I}_N \partial_x (U_N)^{p+1} \right\|_{L^2} &\leq Ch^m \left\| \partial_x (U_N)^{p+1} \right\|_{H^m} \leq Ch^m \|u_e\|_{H^1}^p \|u_e\|_{H^{m+1}}. \end{aligned}$$

Then, using (3.8)–(3.10) and (3.13), we conclude that U_N satisfies (1.1) with a truncation error of spectral accuracy $\mathcal{O}(h^m)$, i.e.,

$${}_a^c D_t^\alpha U_N + (U_N)^p (U_N)_x - \beta (U_N)_{xx} + \gamma (U_N)_{xxx} = F_N + r_0, \tag{3.14}$$

in which $\|r_0\|_2 \leq Ch^m$.

3.2 Analysis of truncation error in time

Let \mathcal{I} be the discrete interpolation operator. For the approximate solution $U_N^n = U_N(x, t_n)$ define its vector grid function $\mathbf{U}^n = \mathcal{I}U_N^n$ as its discrete interpolation.

Theorem 3.1 *Suppose the unique periodic solution of (1.1) satisfies the following regularity assumption*

$$u_e \in H^2(0, T; L^2) \cap L^\infty(0, T; H^{m+1}) \cap H^1(0, T; H^2).$$

Then, we have

$$\mu \left[a_0 \mathbf{U}^n - \sum_{k=1}^{n-1} (a_{n-k-1} - a_{n-k}) \mathbf{U}^k - a_{n-1} \mathbf{U}^0 \right] - \beta \mathcal{D}_N^2 \mathbf{U}^n + \tag{3.15}$$

$$\gamma \mathcal{D}_N^4 \mathbf{U}^n + \frac{1}{p+1} \mathcal{D}_N \left(\mathbf{U}^{n-1} \right)^{p+1} = \mathbf{F}^n + \mathbf{r}^n,$$

in which \mathbf{r}^n satisfies

$$\|\mathbf{r}\|_{l^2(0, T; l^2)} = \left(\tau \sum_{k=0}^M \|\mathbf{r}^k\|_2^2 \right)^{1/2} \leq C(\tau + h^m),$$

and \mathbf{F} is discrete interpolation of F_N .

Proof Let us consider the operator A as

$$A(\mathbf{U}^n) = \mu \left[a_0 \mathbf{U}^n - \sum_{k=1}^{n-1} (a_{n-k-1} - a_{n-k}) \mathbf{U}^k - a_{n-1} \mathbf{U}^0 \right].$$

From Lemma 2.1, we have

$$A(U_N^n) = {}^c D_\alpha^t (U_N^n) + r_1^n(\cdot),$$

in which

$$\|r_1^n\|_{L_2} \leq C\tau^{2-\alpha} \|U_N(\cdot)\|_{H^2(0, T; L_2)} \leq C\tau^{2-\alpha} \|u_e\|_{H^2(0, T; L_2)}. \tag{3.16}$$

Therefore,

$$\|A(\mathbf{U}^n) - \mathcal{I}({}^c D_\alpha^t (U_N^n))\|_2 = \|A(U_N^n) - {}^c D_\alpha^t (U_N^n)\|_{L_2} \leq C\tau^{2-\alpha} \|u_e\|_{H^2(0, T; L_2)}.$$

Note that $\|\mathbf{F}^n - \mathcal{I}F_N^n\|_2 = 0$, and since $U_N^n \in \mathcal{B}^N$ we have

$$\|\mathcal{D}_N^2 \mathbf{U}^n - \mathcal{I}(\partial_x^2 U_N^n)\|_2 = 0,$$

$$\|\mathcal{D}_N^4 \mathbf{U}^n - \mathcal{I}(\partial_x^4 U_N^n)\|_2 = 0.$$

For the nonlinear term, we can write

$$\begin{aligned}
 \left\| \mathcal{D}_N \left(U_N^{n-1} \right)^{p+1} - \mathcal{I} \partial_x \left(\left(U_N^{n-1} \right)^{p+1} \right) \right\|_2 &= \left\| \partial_x \mathcal{I}_N \left(U_N^{n-1} \right)^{p+1} - \mathcal{I}_N \partial_x \left(U_N^{n-1} \right)^{p+1} \right\|_{L^2} \\
 &\leq \left\| \partial_x \mathcal{I}_N \left(U_N^{n-1} \right)^{p+1} - \partial_x \left(U_N^{n-1} \right)^{p+1} \right\|_{L^2} \\
 &\quad + \left\| \partial_x \left(U_N^{n-1} \right)^{p+1} - \mathcal{I}_N \partial_x \left(U_N^{n-1} \right)^{p+1} \right\|_{L^2} \\
 &\leq \left\| \mathcal{I}_N \left(U_N^{n-1} \right)^{p+1} - \left(U_N^{n-1} \right)^{p+1} \right\|_{H^1} \\
 &\quad + Ch^m \left\| \partial_x \left(U_N^{n-1} \right)^{p+1} \right\|_{H^m} \\
 &\leq Ch^m \left\| \left(U_N^{n-1} \right)^{p+1} \right\|_{H^{m+1}} \\
 &\leq Ch^m \|U_N\|_{L^\infty(0,T;H^{m+1})}^{p+1}. \tag{3.17}
 \end{aligned}$$

Also from Lemma 2.5, we have

$$\frac{1}{p+1} \partial_x \left(\left(U_N^{n-1} \right)^{p+1} \right) - \left(U_N^n \right)^p \partial_x U_N^n = r_2^n(\cdot) = -\tau \left(\partial_{tx} \left(U_N^n \right)^{p+1} \right) + \mathcal{O}(\tau^2),$$

so

$$\begin{aligned}
 \left\| \mathcal{I} \left(\frac{1}{p+1} \partial_x \left(\left(U_N^{n-1} \right)^{p+1} \right) - \left(U_N^n \right)^p \partial_x U_N^n \right) \right\|_2 &\leq C\tau \left\| \mathcal{I}_N \left(\partial_{tx} \left(U_N^n \right)^{p+1} \right) \right\|_{L^2} \\
 &\leq C\tau \left\| \partial_t \left(U_N^n \right)^{p+1} \right\|_{H^2} \\
 &\leq C\tau \|U_N\|_{H^1(0,T;H^2)}^{p+1} \\
 &\leq C\tau \|u_e\|_{H^1(0,T;H^2)}^{p+1}, \tag{3.18}
 \end{aligned}$$

which gives

$$\|r_2\|_{l^2(0,T;l^2)} \leq C\tau \|u_e\|_{H^1(0,T;H^2)}^{p+1}. \tag{3.19}$$

Then, from the analysis of truncation error of U_N in (3.14) and $r = r_0 + r_1 + r_2$, the proof is completed. \square

Theorem 3.2 *Suppose the unique periodic solution of (1.1) satisfies the following regularity assumption*

$$u_e \in H^2(0, T; H^1) \cap L^\infty(0, T; H^{m+1}) \cap H^1(0, T; H^2).$$

Then, for the Scheme II, we have

$$\begin{aligned} & \mu \left[a_0 \left(\frac{\mathbf{U}^n + \mathbf{U}^{n-1}}{2} \right) - \sum_{k=1}^{n-1} (a_{n-k-1} - a_{n-k}) \left(\frac{\mathbf{U}^k + \mathbf{U}^{k-1}}{2} \right) - a_{n-1} \mathbf{U}^0 \right] \\ & - \beta \mathcal{D}_N^2 \left(\frac{3}{4} \mathbf{U}^n + \frac{1}{4} \mathbf{U}^{n-2} \right) + \gamma \mathcal{D}_N^4 \left(\frac{3}{4} \mathbf{U}^n + \frac{1}{4} \mathbf{U}^{n-2} \right) \\ & + \frac{1}{p+1} \mathcal{D}_N \left(\frac{3}{2} (\mathbf{U}^{n-1})^{p+1} - \frac{1}{2} (\mathbf{U}^{n-2})^{p+1} \right) = \left(\frac{3}{4} \mathbf{F}^n + \frac{1}{4} \mathbf{F}^{n-2} \right) + \mathbf{r}^{n-\frac{1}{2}}, \end{aligned} \tag{3.20}$$

in which

$$\|\mathbf{r}\|_{L^2(0,T;L^2)} \leq C(\tau^{2-\alpha} + h^m).$$

Proof The proof can be followed in a similar manner as previous Theorem. □

4 Stability and convergence analysis of Scheme I

Let \mathbf{u}^n be the vector of grid values of numerical solution at n th time level, and $\mathbf{e}_i^n = \mathbf{U}_i^n - \mathbf{u}_i^n$ be the point-wise error function at i th grid. Then, with the interpolation formula given by (2.3) in view of (2.5), i.e., $u_N^n = \mathcal{I}_N \mathbf{u}^n$ and $e_N^n = \mathcal{I}_N \mathbf{e}^n$, the continuous solution function $u_N^n \in \mathcal{B}^N$, and continuous error function $e_N^n \in \mathcal{B}^N$ are obtained, respectively.

Regarding the regularity of the constructed solution, we suppose that U_N belongs to the sobolev space $W^{2,\infty}$ so, we have

$$\|U_N\|_{L^\infty(0,T;W^{2,\infty})} \leq C^*, \text{ i.e. } \|U_N^n\|_{L^\infty} \leq C^*, \|(U_N^n)_x\|_{L^\infty} \leq C^*, \|(U_N^n)_{xx}\|_{L^\infty} \leq C^*. \tag{4.1}$$

Theorem 4.1 *For any fixed time T , assume that the exact solution u_e for the fractional equation (1.1) belongs to $H^2(0, T; L^2) \cap L^\infty(0, T; H^{m+1}) \cap H^1(0, T; H^2)$ and $f \in L^\infty(0, T; H^m)$. Let $u_{\tau,h}$ be the continuous extension of the fully discrete numerical solution obtained by scheme (2.9). Then as $h, \tau \rightarrow 0$, we have the following convergence result:*

$$\|u_{\tau,h} - u_e\|_{L^\infty(0,T;H^2)} \leq \tilde{C} (\tau + h^m). \tag{4.2}$$

Proof We start by assuming a priori that the numerical error function has an H^2 bound at time step t_{n-1} [14]:

$$\|e_N^{n-1}\|_{H^2} \leq 1, \text{ with } e_N^{n-1} = \mathcal{I}_N \mathbf{e}^{n-1},$$

which yields directly the following results, using 1D Sobolev embedding,

$$\begin{aligned} \|u_N^{n-1}\|_{H^2} &= \|U_N^{n-1} - e_N^{n-1}\|_{H^2} \leq C^* + 1 = C_1, \\ \|u^{n-1}\|_{\infty} &\leq C \|u_N^{n-1}\|_{L^\infty} \leq C \|u_N^{n-1}\|_{H^2} \leq CC_1 = C_2. \end{aligned} \tag{4.3}$$

Subtracting (2.9) from (3.15), with operator A as in Theorem 3.1, yields

$$A(\mathbf{e}^n) - \beta \mathcal{D}_N^2 \mathbf{e}^n + \gamma \mathcal{D}_N^4 \mathbf{e}^n + \frac{1}{p+1} \left[\mathcal{D}_N(\mathbf{U}^{n-1})^{p+1} - \mathcal{D}_N(\mathbf{u}^{n-1})^{p+1} \right] = \mathbf{F}^n - \mathbf{f}^n + \mathbf{r}^n. \tag{4.4}$$

Let

$$A_1 = \frac{1}{p+1} \left[\mathcal{D}_N(\mathbf{U}^{n-1})^{p+1} - \mathcal{D}_N(\mathbf{u}^{n-1})^{p+1} \right].$$

Then, taking an l^2 inner product of (4.4) with \mathbf{e}^n gives

$$\begin{aligned} \mu \left[a_0 \langle \mathbf{e}^n, \mathbf{e}^n \rangle - \sum_{k=1}^{n-1} (a_{n-k-1} - a_{n-k}) \langle \mathbf{e}^k, \mathbf{e}^n \rangle - a_{n-1} \langle \mathbf{e}^0, \mathbf{e}^n \rangle \right] - \beta \langle \mathcal{D}_N^2 \mathbf{e}^n, \mathbf{e}^n \rangle \\ + \gamma \langle \mathcal{D}_N^4 \mathbf{e}^n, \mathbf{e}^n \rangle + \langle A_1, \mathbf{e}^n \rangle = \langle \mathbf{F}^n - \mathbf{f}^n, \mathbf{e}^n \rangle + \langle \mathbf{r}^n, \mathbf{e}^n \rangle. \end{aligned} \tag{4.5}$$

For each positive number ϵ , using inequality $ab \leq \epsilon a^2 + \frac{1}{4\epsilon} b^2$, we can write

$$\langle \mathbf{r}^n, \mathbf{e}^n \rangle \leq \frac{1}{\mu a_{n-1}} \|\mathbf{r}^n\|_2^2 + \frac{\mu a_{n-1}}{4} \|\mathbf{e}^n\|_2^2. \tag{4.6}$$

Based on (2.7), and the regularity of constructed solution (4.1), and the a priori assumptions (4.3), we have

$$\begin{aligned} \langle A_1, \mathbf{e}^n \rangle &= \frac{h}{p+1} \sum_{j=0}^{2N} \left[\mathcal{D}_N(\mathbf{U}^{n-1})^{p+1} - \mathcal{D}_N(\mathbf{u}^{n-1})^{p+1} \right]_j \mathbf{e}_j^n \\ &= -\frac{h}{p+1} \sum_{j=0}^{2N} \left[(\mathbf{U}^{n-1})^{p+1} - (\mathbf{u}^{n-1})^{p+1} \right]_j (\mathcal{D}_N \mathbf{e}^n)_j \\ &= -\frac{h}{p+1} \sum_{j=0}^{2N} \left(\mathbf{e}_j^{n-1} \sum_{k=1}^p (\mathbf{U}_j^{n-1})^{p-k} (\mathbf{u}_j^{n-1})^k \right) (\mathcal{D}_N \mathbf{e}^n)_j \\ &\leq Ch \sum_{j=0}^{2N} |\mathbf{e}_j^{n-1}| |(\mathcal{D}_N \mathbf{e}^n)_j| \leq C \left(\frac{C}{2\beta} \|\mathbf{e}^{n-1}\|_2^2 + \frac{\beta}{2C} \|\mathcal{D}_N \mathbf{e}^n\|_2^2 \right) \\ &= \frac{C^2}{2\beta} \|\mathbf{e}^{n-1}\|_2^2 + \frac{\beta}{2} \|\mathcal{D}_N \mathbf{e}^n\|_2^2. \end{aligned} \tag{4.7}$$

Substituting (4.6)–(4.7) in (4.5) and using (2.7), we get

$$\begin{aligned}
 \mu \|\mathbf{e}^n\|_2^2 + \beta \|\mathcal{D}_N \mathbf{e}^n\|_2^2 + \gamma \|\mathcal{D}_N^2 \mathbf{e}^n\|_2^2 &\leq \mu \sum_{k=1}^{n-1} (a_{n-k-1} - a_{n-k}) \langle \mathbf{e}^k, \mathbf{e}^n \rangle + \mu a_{n-1} \langle \mathbf{e}^0, \mathbf{e}^n \rangle \\
 &\quad + \frac{1}{\mu a_{n-1}} \|\mathbf{r}^n\|_2^2 + \frac{C^2}{2\beta} \|\mathbf{e}^{n-1}\|_2^2 + \frac{\mu a_{n-1}}{4} \|\mathbf{e}^n\|_2^2 \\
 &\quad + \frac{\beta}{2} \|\mathcal{D}_N \mathbf{e}^n\|_2^2 + \langle \mathbf{F}^n - \mathbf{f}^n, \mathbf{e}^n \rangle \\
 &\leq \frac{\mu}{2} \sum_{k=1}^{n-1} (a_{n-k-1} - a_{n-k}) \left(\|\mathbf{e}^k\|_2^2 + \|\mathbf{e}^n\|_2^2 \right) \\
 &\quad + \mu a_{n-1} \left(2\|\mathbf{e}^0\|_2^2 + \frac{1}{8} \|\mathbf{e}^n\|_2^2 \right) + \frac{1}{\mu a_{n-1}} \|\mathbf{r}^n\|_2^2 \\
 &\quad + \frac{C^2}{2\beta} \|\mathbf{e}^{n-1}\|_2^2 + \frac{\mu a_{n-1}}{4} \|\mathbf{e}^n\|_2^2 + \frac{\beta}{2} \|\mathcal{D}_N \mathbf{e}^n\|_2^2 \\
 &\quad + \frac{\mu a_{n-1}}{8} \|\mathbf{e}^n\|_2^2 + \frac{2}{\mu a_{n-1}} \|\mathbf{F}^n - \mathbf{f}^n\|_2^2 \\
 &= \frac{\mu}{2} \sum_{k=1}^{n-1} (a_{n-k-1} - a_{n-k}) \|\mathbf{e}^k\|_2^2 + 2\mu a_{n-1} \|\mathbf{e}^0\|_2^2 \\
 &\quad + \mu \left(\frac{1}{2} - \frac{1}{4} a_{n-1} \right) \|\mathbf{e}^n\|_2^2 \\
 &\quad + \frac{1}{\mu a_{n-1}} \|\mathbf{r}^n\|_2^2 + \frac{C^2}{2\beta} \|\mathbf{e}^{n-1}\|_2^2 + \frac{\mu a_{n-1}}{4} \|\mathbf{e}^n\|_2^2 \\
 &\quad + \frac{\beta}{2} \|\mathcal{D}_N \mathbf{e}^n\|_2^2 + \frac{2}{\mu a_{n-1}} \|\mathbf{F}^n - \mathbf{f}^n\|_2^2.
 \end{aligned}$$

Using

$$\|\mathbf{F}^n - \mathbf{f}^n\|_2 = \|\mathcal{I}F_N^n - \mathbf{f}^n\|_2 = \|\mathcal{P}_N f^n - f^n + f^n - \mathcal{I}_N \mathbf{f}^n\|_{L^2} \leq C \|f^n\|_{H^m} h^m,$$

we then obtain

$$\begin{aligned}
 \mu \|\mathbf{e}^n\|_2^2 + \beta \|\mathcal{D}_N \mathbf{e}^n\|_2^2 + 2\gamma \|\mathcal{D}_N^2 \mathbf{e}^n\|_2^2 &\leq \mu \sum_{k=1}^{n-1} (a_{n-k-1} - a_{n-k}) \|\mathbf{e}^k\|_2^2 \\
 &\quad + \frac{C^2}{\beta} \|\mathbf{e}^{n-1}\|_2^2 + C(\tau + h^m)^2,
 \end{aligned}$$

or

$$\begin{aligned}
 \|\mathbf{e}^n\|_2^2 + \beta \mu^{-1} \|\mathcal{D}_N \mathbf{e}^n\|_2^2 + 2\gamma \mu^{-1} \|\mathcal{D}_N^2 \mathbf{e}^n\|_2^2 &\leq \sum_{k=1}^{n-1} (a_{n-k-1} - a_{n-k}) \|\mathbf{e}^k\|_2^2 \\
 &\quad + \frac{C^2 \mu^{-1}}{\beta} \|\mathbf{e}^{n-1}\|_2^2 + C \mu^{-1} (\tau + h^m)^2.
 \end{aligned}
 \tag{4.8}$$

Note that in the last equation, we use the fact that $\|\mathbf{e}^0\|_{H^1} \leq Ch^m$ due to the collocation spectral approximation of the initial data. Also $\mu^{-1} = \tau^\alpha \Gamma(2 - \alpha)$ is always bounded. Then, using Gronwall’s Lemma 2.2 and (4.8), we obtain

$$\begin{aligned} & \|\mathbf{e}^n\|_2^2 + \beta\mu^{-1} \|\mathcal{D}_N \mathbf{e}^n\|_2^2 + 2\gamma\mu^{-1} \|\mathcal{D}_N^2 \mathbf{e}^n\|_2^2 \\ & \leq C\mu^{-1}(\tau + h^m)^2 \exp\left(\sum_{k=1}^{n-1} (a_{n-k-1} - a_{n-k})\right) \leq C(\tau + h^m)^2, \end{aligned} \tag{4.9}$$

so

$$\|e_N^n\|_{H^2} \leq C^{**}(\tau + h^m). \tag{4.10}$$

Finally, the proof is fully established with just recalling that the a priori assumed bound (4.3) holds inductively.

Recovery of the H^2 a priori assumed bound (4.3) Obviously, using this $l^\infty(0, T; H^2)$ error estimate, (4.10), it can be obtained that the a priori assumed H^2 bound (4.3) is also valid for the numerical error vector \mathbf{e}^n at time step t^n , provided

$$\tau \leq (C^{**})^{-1}, \quad h \leq (C^{**})^{-m}.$$

□

5 Stability and convergence analysis of Scheme II

Theorem 5.1 *For any fixed time T , assume that the exact solution u_e for the fractional equation (1.1) satisfies $u_e \in L^\infty(0, T; H^{m+1}) \cap H^3(0, T; H^2)$ and $f \in L^\infty(0, T; H^m)$. Let $u_{\tau,h}$ be the continuous extension of the fully discrete numerical solution of proposed scheme (2.9). Then as $h, \tau \rightarrow 0$, we have the following convergence result:*

$$\|u_{\tau,h} - u_e\|_{l^\infty(0,T;H^2)} \leq \tilde{C} \left(\tau^{2-\alpha} + h^m\right). \tag{5.1}$$

Proof We again start by assuming a priori that the numerical error function has an H^2 bound at time steps t_{n-1}, t_{n-2} , which implies that (4.3) holds for t_{n-1}, t_{n-2} . Subtracting (2.10) from (3.20) yields

$$\begin{aligned} & A \left(\frac{\mathbf{e}^n + \mathbf{e}^{n-1}}{2}\right) - \beta\mathcal{D}_N^2 \left(\frac{3}{4}\mathbf{e}^n + \frac{1}{4}\mathbf{e}^{n-2}\right) + \gamma\mathcal{D}_N^4 \left(\frac{3}{4}\mathbf{e}^n + \frac{1}{4}\mathbf{e}^{n-2}\right) \\ & + \frac{1}{p+1} \mathcal{D}_N \left[\left(\frac{3}{2}(\mathbf{U}^{n-1})^{p+1} - \frac{1}{2}(\mathbf{U}^{n-2})^{p+1}\right) \right. \\ & \quad \left. - \left(\frac{3}{2}(\mathbf{u}^{n-1})^{p+1} - \frac{1}{2}(\mathbf{u}^{n-2})^{p+1}\right) \right] \\ & = \frac{3}{4}(\mathbf{F}^n - \mathbf{f}^n) + \frac{1}{4}(\mathbf{F}^{n-2} - \mathbf{f}^{n-2}) + \mathbf{r}^{n-\frac{1}{2}}. \end{aligned} \tag{5.2}$$

Let

$$A_2 = \frac{1}{p+1} \mathcal{D}_N \left[\left(\frac{3}{2} (\mathbf{U}^{n-1})^{p+1} - \frac{1}{2} (\mathbf{U}^{n-2})^{p+1} \right) - \left(\frac{3}{2} (\mathbf{u}^{n-1})^{p+1} - \frac{1}{2} (\mathbf{u}^{n-2})^{p+1} \right) \right].$$

Taking an l^2 inner product of (5.2) with \mathbf{e}^n gives

$$\begin{aligned} & \mu \left[a_0 \left\langle \frac{\mathbf{e}^n + \mathbf{e}^{n-1}}{2}, \mathbf{e}^n \right\rangle - \sum_{k=1}^{n-1} (a_{n-k-1} - a_{n-k}) \left\langle \frac{\mathbf{e}^k + \mathbf{e}^{k-1}}{2}, \mathbf{e}^n \right\rangle - a_{n-1} \langle \mathbf{e}^0, \mathbf{e}^n \rangle \right] \\ & - \beta \left\langle \mathcal{D}_N^2 \frac{3\mathbf{e}^n + \mathbf{e}^{n-2}}{4}, \mathbf{e}^n \right\rangle + \gamma \left\langle \mathcal{D}_N^4 \frac{3\mathbf{e}^n + \mathbf{e}^{n-2}}{4}, \mathbf{e}^n \right\rangle + \langle A_2, \mathbf{e}^n \rangle \\ & = \frac{3}{4} \langle \mathbf{F}^n - \mathbf{f}^n, \mathbf{e}^n \rangle + \frac{1}{4} \langle \mathbf{F}^{n-2} - \mathbf{f}^{n-2}, \mathbf{e}^n \rangle + \langle \mathbf{r}^{n-\frac{1}{2}}, \mathbf{e}^n \rangle. \end{aligned} \tag{5.3}$$

We can write

$$\langle \mathbf{r}^{n-\frac{1}{2}}, \mathbf{e}^n \rangle \leq \frac{2}{\mu a_{n-1}} \|\mathbf{r}^{n-\frac{1}{2}}\|_2^2 + \frac{\mu a_{n-1}}{8} \|\mathbf{e}^n\|_2^2, \tag{5.4}$$

and

$$\begin{aligned} \langle A_2, \mathbf{e}^n \rangle &= \frac{1}{p+1} \left\langle \mathcal{D}_N \left[\left(\frac{3}{2} (\mathbf{U}^{n-1})^{p+1} - \frac{1}{2} (\mathbf{U}^{n-2})^{p+1} \right) - \left(\frac{3}{2} (\mathbf{u}^{n-1})^{p+1} - \frac{1}{2} (\mathbf{u}^{n-2})^{p+1} \right) \right], \mathbf{e}^n \right\rangle \\ &= -\frac{1}{p+1} \left\langle \frac{3}{2} \left((\mathbf{U}^{n-1})^{p+1} - (\mathbf{u}^{n-1})^{p+1} \right) - \frac{1}{2} \left((\mathbf{U}^{n-2})^{p+1} - (\mathbf{u}^{n-2})^{p+1} \right), \mathcal{D}_N \mathbf{e}^n \right\rangle \\ &= -\frac{h}{p+1} \sum_{j=0}^{2N} \left[\frac{3}{2} \left(\mathbf{e}_j^{n-1} \sum_{k=1}^p (\mathbf{U}_j^{n-1})^{p-k} (\mathbf{u}_j^{n-1})^k \right) - \frac{1}{2} \left(\mathbf{e}_j^{n-2} \sum_{k=1}^p (\mathbf{U}_j^{n-2})^{p-k} (\mathbf{u}_j^{n-2})^k \right) \right] (\mathcal{D}_N \mathbf{e}^n)_j \\ &\leq Ch \sum_{j=0}^{2N} \left(|\mathbf{e}_j^{n-1}| + |\mathbf{e}_j^{n-2}| \right) |(\mathcal{D}_N \mathbf{e}^n)_j| \\ &\leq C \left(\frac{2C}{\beta} \|\mathbf{e}^{n-1}\|_2^2 + \frac{2C}{\beta} \|\mathbf{e}^{n-2}\|_2^2 + \frac{\beta}{4C} \|\mathcal{D}_N \mathbf{e}^n\|_2^2 \right) \\ &= \frac{2C^2}{\beta} \left(\|\mathbf{e}^{n-1}\|_2^2 + \|\mathbf{e}^{n-2}\|_2^2 \right) + \frac{\beta}{4} \|\mathcal{D}_N \mathbf{e}^n\|_2^2. \end{aligned} \tag{5.5}$$

Substituting (5.4)–(5.5) in (5.3), we obtain

$$\begin{aligned}
 2\mu \|\mathbf{e}^n\|_2^2 + 3\beta \|\mathcal{D}_N \mathbf{e}^n\|_2^2 + 3\gamma \|\mathcal{D}_N^2 \mathbf{e}^n\|_2^2 &\leq 2\mu \sum_{k=1}^{n-1} (a_{n-k-1} - a_{n-k}) \left(\|\mathbf{e}^k, \mathbf{e}^n\| + \|\mathbf{e}^{k-1}, \mathbf{e}^n\| \right) \\
 &+ 4\mu a_{n-1} \|\mathbf{e}^0, \mathbf{e}^n\| + \frac{8}{\mu a_{n-1}} \|\mathbf{r}^{n-\frac{1}{2}}\|_2^2 + \frac{\mu a_{n-1}}{2} \|\mathbf{e}^n\|_2^2 + \frac{8C^2}{\beta} \|\mathbf{e}^{n-1}\|_2^2 \\
 &+ \frac{8C^2}{\beta} \|\mathbf{e}^{n-2}\|_2^2 \\
 &+ \beta \|\mathcal{D}_N \mathbf{e}^n\|_2^2 + \frac{\beta}{4} \|\mathcal{D}_N \mathbf{e}^{n-2}\|_2^2 + \beta \|\mathcal{D}_N \mathbf{e}^n\|_2^2 + \frac{\gamma}{8} \|\mathcal{D}_N^2 \mathbf{e}^{n-2}\|_2^2 + 2\gamma \|\mathcal{D}_N^2 \mathbf{e}^n\|_2^2 \\
 &+ 3 \langle \mathbf{F}^n - \mathbf{f}^n, \mathbf{e}^n \rangle + \langle \mathbf{F}^{n-2} - \mathbf{f}^{n-2}, \mathbf{e}^n \rangle \\
 &\leq \mu \sum_{k=1}^{n-1} (a_{n-k-1} - a_{n-k}) \left(2\|\mathbf{e}^k\|_2^2 + 2\|\mathbf{e}^{k-1}\|_2^2 + \|\mathbf{e}^n\|_2^2 \right) \\
 &+ \mu a_{n-1} \left(16\|\mathbf{e}^0\|_2^2 + \frac{1}{4}\|\mathbf{e}^n\|_2^2 \right) + \frac{8}{\mu a_{n-1}} \|\mathbf{r}^{n-\frac{1}{2}}\|_2^2 + \frac{\mu a_{n-1}}{2} \|\mathbf{e}^n\|_2^2 \\
 &+ \frac{8C^2}{\beta} \|\mathbf{e}^{n-1}\|_2^2 \\
 &+ \frac{8C^2}{\beta} \|\mathbf{e}^{n-2}\|_2^2 + \beta \|\mathcal{D}_N \mathbf{e}^n\|_2^2 + \frac{\beta}{4} \|\mathcal{D}_N \mathbf{e}^{n-2}\|_2^2 + \beta \|\mathcal{D}_N \mathbf{e}^n\|_2^2 + \frac{\gamma}{8} \|\mathcal{D}_N^2 \mathbf{e}^{n-2}\|_2^2 \\
 &+ 2\gamma \|\mathcal{D}_N^2 \mathbf{e}^n\|_2^2 + \frac{\mu a_{n-1}}{4} \|\mathbf{e}^n\|_2^2 + \frac{18}{\mu a_{n-1}} \|\mathbf{F}^n - \mathbf{f}^n\|_2^2 + \frac{2}{\mu a_{n-1}} \|\mathbf{F}^{n-2} - \mathbf{f}^{n-2}\|_2^2.
 \end{aligned}$$

Now, we can write

$$\begin{aligned}
 \left(\mu \|\mathbf{e}^n\|_2^2 + \beta \|\mathcal{D}_N \mathbf{e}^n\|_2^2 + \gamma \|\mathcal{D}_N^2 \mathbf{e}^n\|_2^2 \right) &\leq 2\mu \sum_{k=1}^{n-1} (a_{n-k-1} - a_{n-k}) \left(\|\mathbf{e}^k\|_2^2 + \|\mathbf{e}^{k-1}\|_2^2 \right) \\
 &+ 16\mu a_{n-1} \|\mathbf{e}^0\|_2^2 + \frac{8}{\mu a_{n-1}} \|\mathbf{r}^{n-\frac{1}{2}}\|_2^2 + \frac{8C^2}{\beta} \|\mathbf{e}^{n-1}\|_2^2 + \frac{8C^2}{\beta} \|\mathbf{e}^{n-2}\|_2^2 \\
 &+ \frac{\beta}{4} \|\mathcal{D}_N \mathbf{e}^{n-2}\|_2^2 + \frac{\gamma}{8} \|\mathcal{D}_N^2 \mathbf{e}^{n-2}\|_2^2 + Ch^{2m},
 \end{aligned}$$

or

$$\begin{aligned}
 \|\mathbf{e}^n\|_2^2 + \beta \mu^{-1} \|\mathcal{D}_N \mathbf{e}^n\|_2^2 + \gamma \mu^{-1} \|\mathcal{D}_N^2 \mathbf{e}^n\|_2^2 &\leq 2 \sum_{k=1}^{n-1} (a_{n-k-1} - a_{n-k}) \\
 &\times \left(\|\mathbf{e}^k\|_2^2 + \|\mathbf{e}^{k-1}\|_2^2 \right) \\
 &+ \frac{8C^2}{\beta} \mu^{-1} \|\mathbf{e}^{n-1}\|_2^2 + \frac{8C^2}{\beta} \mu^{-1} \|\mathbf{e}^{n-2}\|_2^2 + \frac{\beta}{4} \mu^{-1} \|\mathcal{D}_N \mathbf{e}^{n-2}\|_2^2 \\
 &+ \frac{\gamma}{8} \mu^{-1} \|\mathcal{D}_N^2 \mathbf{e}^{n-2}\|_2^2 + C \mu^{-1} (\tau^{2-\alpha} + h^m)^2.
 \end{aligned}$$

Using Gronwall’s Lemma 2.2 gives

$$\begin{aligned} & \|e^n\|_2^2 + \beta\mu^{-1} \|D_N e^n\|_2^2 + 2\mu^{-1}\gamma \|D_N^2 e^n\|_2^2 \\ & \leq C\mu^{-1}(\tau^{2-\alpha} + h^m)^2 \exp\left(\sum_{k=1}^{n-1} (a_{n-k-1} - a_{n-k})\right) \leq C(\tau^{2-\alpha} + h^m)^2, \end{aligned}$$

so

$$\|e_N^n\|_{H^2} \leq C^{**}(\tau^{2-\alpha} + h^m). \tag{5.6}$$

Then, the proof is fully established as, from (5.6), it is simply obtained that the a priori assumed bound (4.3) holds inductively. □

Regarding the consistency analysis, regularity of constructed solution (4.1), (4.10), and (5.6), we can state the following corollary on the stability of the proposed schemes.

Corollary 1 *The numerical scheme I, (2.9), and the scheme II, (2.10), are unconditionally stable.*

6 Numerical experiments

In this section, we present the numerical results of the new schemes on several test problems. We tested the accuracy and stability of the schemes described in this paper by performing the mentioned schemes for different values of h and τ . We performed our computations using Matlab 7 software on a Pentium IV, 2800 MHz CPU machine with 2 Gbyte of memory. Also, we have calculated the computational order of the schemes presented in this article (denoted by C-order) with the following formula [29]:

$$\frac{\log(\frac{E_1}{E_2})}{\log(\frac{h_1}{h_2})},$$

in which E_1 and E_2 are errors correspond to grids with mesh size h_1 and h_2 respectively.

Test problem 1 We consider the time fractional (1.1) for $x \in [-2, 2]$, with initial condition

$$u(x, 0) = 0, \tag{6.1}$$

and

$$\begin{aligned} f(x, t) = & \frac{2t^{2-\alpha}}{\Gamma(3-\alpha)} \sin(\pi x) + \pi t^{2p+2} \sin(\pi x)^p \cos(\pi x) + \pi^2 \beta t^2 \sin(\pi x) \\ & + \pi^4 \gamma t^2 \sin(\pi x). \end{aligned} \tag{6.2}$$

The exact solution of this problem is $u(x, t) = t^2 \sin(\pi x)$. We solve this problem with the proposed schemes in this paper for two cases $\gamma = 0$ and $\gamma \neq 0$. Also for this test problem, we set $T = 1$.

Case I : $\gamma = 0$

If in (1.1), we put $\gamma = 0$, the following generalized time fractional Burgers equation is resulted

$${}_0^c D_t^\alpha u(x, t) + u^p u_x - \beta u_{xx} = f(x, t). \tag{6.3}$$

We consider this equation with conditions (6.1) and (6.2). For this problem, beside to the proposed schemes in paper, we also implemented the linear implicit finite difference scheme presented in [25], given with following formula

$$a_0 u_j^n - \sum_{k=1}^{n-1} (a_{n-k-1} - a_{n-k}) u_j^k - a_{n-1} u_j^0 = \beta \mu^{-1} (u_j^n)_{x\bar{x}} - \frac{\mu^{-1}}{p+2} \left[(u_j^{n-1})^p (u_j^n)_{\hat{x}} + ((u_j^{n-1})^p u_j^n)_{\hat{x}} \right]. \tag{6.4}$$

This method needs to solve a tri-diagonal system of algebraic equations $Au = b$ at each time level in which both A and b should be updated at each level. But the linear systems resulted from our proposed schemes (2.9) and (2.10) are diagonal in Fourier space and combining them with fast Fourier transform (FFT) routine, leads to the schemes with less CPU time and will be confirmed by numerical implementation. Beside this, updating scheme (6.4) for the solution of time fractional equation (1.1) (with $\gamma \neq 0$), resulted to a penta-diagonal system which is more expensive.

We put $\beta = p = 1$ and show the CPU time (s) and l^2 -error of proposed schemes I and II with $N = 16$ and method of [25] with $N = 500$ for different values of α and τ in Tables 1 and 2.

Table 1 Comparison of C-order, CPU time (s) and l^2 -error for Test problem 1 with $\alpha = 0.7$

τ	Scheme I			Method of [25]		
	l^2 -error	CPU time	C-order	l^2 -error	CPU time	C-order
1/10	9.4380×10^{-3}	0.0031	–	2.7389×10^{-3}	0.4555	–
1/20	5.0332×10^{-3}	0.0053	0.9070	1.3741×10^{-3}	0.8717	0.9951
1/50	2.0883×10^{-3}	0.0146	0.9601	5.5651×10^{-4}	2.2129	0.9864
1/100	1.0556×10^{-3}	0.0233	0.9843	2.8484×10^{-4}	4.1571	0.9663
1/500	2.1253×10^{-4}	0.1979	0.9959	7.2784×10^{-5}	23.7387	0.8478
1/1000	1.0629×10^{-4}	0.6494	0.9997	5.0030×10^{-5}	47.3176	0.5408
1/2000	5.3134×10^{-5}	2.3198	1.0003	4.0776×10^{-5}	103.5368	0.2951

Table 2 Comparison of C-order, CPU time (s) and l^2 -error for Test problem 1 with $\alpha = 0.2$

τ	Scheme II			Method of [25]		
	l^2 -error	CPU time	C-order	l^2 -error	CPU time	C-order
1/5	7.9956×10^{-3}	0.0025	—	5.4806×10^{-3}	0.2307	—
1/10	2.2720×10^{-3}	0.0056	1.8152	2.7430×10^{-3}	0.4219	0.9985
1/15	1.0496×10^{-3}	0.0093	1.9046	1.8317×10^{-3}	0.7200	0.9959
1/30	2.7289×10^{-4}	0.0131	1.9120	9.2130×10^{-4}	1.4087	0.9914
1/80	3.9490×10^{-5}	0.0297	1.9708	3.5344×10^{-4}	3.4099	0.9768
1/200	6.4273×10^{-6}	0.0871	1.9814	1.5087×10^{-4}	8.8447	0.9291
1/500	1.0448×10^{-6}	0.3183	1.9827	7.3265×10^{-5}	23.1248	0.7883
1/800	4.1173×10^{-7}	0.6895	1.9813	5.5801×10^{-5}	37.5429	0.5793
1/1500	1.1869×10^{-7}	2.0836	1.9787	4.4043×10^{-5}	71.6557	0.3764
1/3000	3.0196×10^{-8}	7.6103	1.9748	3.8684×10^{-5}	162.7427	0.1872

Tables 1 and 2 confirm that the proposed schemes I and II are more efficient and have good results in terms of both accuracy and CPU time. We fix the spatial resolution ($N = 32$) and show the computational order of proposed schemes I and II in time component for different values of α with $p = 3$, $\beta = 2$ in Table 3.

Table 3 Computational order of proposed schemes in time variable for Test problem 1

α	τ	Scheme I		Scheme II	
		l^2 -error	C-order	l^2 -error	C-order
0.1	1/20	2.3494×10^{-3}	—	6.1841×10^{-4}	—
	1/40	1.2794×10^{-3}	0.8768	1.6940×10^{-4}	1.8681
	1/80	6.6783×10^{-4}	0.9379	4.4153×10^{-5}	1.9399
	1/160	3.4119×10^{-4}	0.9689	1.1260×10^{-5}	1.9713
	1/320	1.7245×10^{-4}	0.9844	2.8428×10^{-6}	1.9858
	1/640	8.6691×10^{-5}	0.9922	7.1426×10^{-7}	1.9928
	1/1280	4.3463×10^{-5}	0.9961	1.7903×10^{-7}	1.9962
0.9	1/50	1.0694×10^{-3}	—	4.3473×10^{-4}	—
	1/100	5.4517×10^{-4}	0.9720	1.9876×10^{-4}	1.1291
	1/200	2.7443×10^{-4}	0.9903	9.2140×10^{-5}	1.1091
	1/400	1.3730×10^{-4}	0.9991	4.2907×10^{-5}	1.1026
	1/800	6.8495×10^{-5}	1.0033	2.0007×10^{-5}	1.1007
	1/1600	3.4132×10^{-5}	1.0049	9.3325×10^{-6}	1.1002

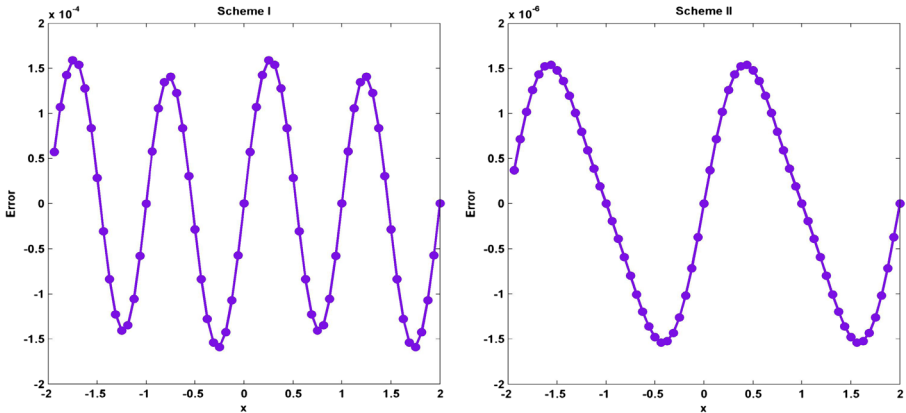


Fig. 1 Plots of obtained errors for Schemes I and II in solving Test problem 1 with $\gamma = 0$

As we see from Table 3, the order of Scheme I in time variable is approximately 1 for both values $\alpha = 0.1$ and $\alpha = 0.9$ which is in good agreement with theoretical results. Also the order of Scheme II for $\alpha = 0.1$ is approximately 1.9 and for $\alpha = 0.9$ is 1.1 which again are compatible with theoretical order $\mathcal{O}(\tau^{2-\alpha})$. Figure 1 shows the error obtained with schemes I and II with $\gamma = 0$, $p = \beta = 1$, $N = 64$, $\tau = 0.001$ and $\alpha = 0.5$ for Test problem 1.

Case II : $\gamma \neq 0$

In this case, we consider the time fractional KS (1.1) with conditions (6.1) and (6.2). In Tables 4 and 5, we present the l^2 -error, CPU time, and computational orders of Schemes I and II with $N = 32$, $p = \beta = \gamma = 1$ and different values of α and τ .

As we see the proposed Schemes I and II need to less CPU time and computational orders are compatible with theoretical orders. To investigate the spectral accuracy in space, we put $\tau = 0.001$ and solve the problem with different values of N . Figure 2

Table 4 Numerical results of proposed schemes in time variable for test problem 1 with $\alpha = 0.2$

τ	Scheme I			Scheme II		
	l^2 -error	CPU time	C-order	l^2 -error	CPU time	C-order
1/10	2.3963×10^{-4}	0.0033	—	7.3203×10^{-5}	0.0096	—
1/20	1.2900×10^{-4}	0.0086	0.8934	1.9523×10^{-5}	0.0120	1.9067
1/40	6.6931×10^{-5}	0.0126	0.9466	5.1461×10^{-6}	0.0194	1.9236
1/80	3.4091×10^{-5}	0.0226	0.9733	1.3525×10^{-6}	0.0366	1.9279
1/160	1.7204×10^{-5}	0.0458	0.9866	3.5630×10^{-7}	0.0805	1.9245
1/320	8.6420×10^{-6}	8.6420	0.9933	9.4335×10^{-8}	0.2212	1.9172

Table 5 Numerical results of proposed schemes in time variable for test problem 1 with $\alpha = 0.8$

τ	Scheme I			Scheme II		
	l^2 -error	CPU time	C-order	l^2 -error	CPU time	C-order
1/30	1.2249×10^{-4}	0.0103	–	8.5470×10^{-5}	0.0154	–
1/60	5.8511×10^{-5}	0.0175	1.0659	3.7012×10^{-5}	0.0265	1.2074
1/120	2.8049×10^{-5}	0.0342	1.0608	1.6070×10^{-5}	0.0550	1.2036
1/240	1.3515×10^{-5}	0.0797	1.0534	6.9860×10^{-6}	0.1352	1.2018
1/480	6.5480×10^{-6}	0.2299	1.0454	3.0388×10^{-6}	0.3725	1.2010
1/960	3.1898×10^{-5}	0.7405	1.0376	1.3222×10^{-6}	1.1935	1.2006
1/1920	1.5615×10^{-6}	2.6886	1.0305	5.7542×10^{-7}	4.7280	1.2003
1/3840	7.6769×10^{-7}	13.456	1.0243	2.5044×10^{-7}	19.969	1.2002

shows the l^2 -error of Schemes I and II with $\alpha = 0.5$ and different values of $\beta = \gamma$ and N which apparently the spatial spectral accuracy is verified.

Test problem 2:

We consider the time fractional (1.1) for $x \in [-4, 4]$, with initial condition

$$u(x, 0) = \cos(\pi x), \tag{6.5}$$

and

$$f(x, t) = \frac{t^{1-\alpha}}{\Gamma(2-\alpha)} \cos(\pi x) - \pi(t+1)^{p+1} \sin(\pi x) \cos^p(\pi x) + (\pi^2\beta + \pi^4\gamma)(t+1) \cos(\pi x). \tag{6.6}$$

The exact solution of this problem is $u(x, t) = (t+1) \cos(\pi x)$. For this problem, we set $T = 1, p = 2, \beta = \gamma = 3$. Tables 6 and 7 present the results of Schemes I and II with $N = 32, \alpha = 0.5, 0.9$ and different values of τ .

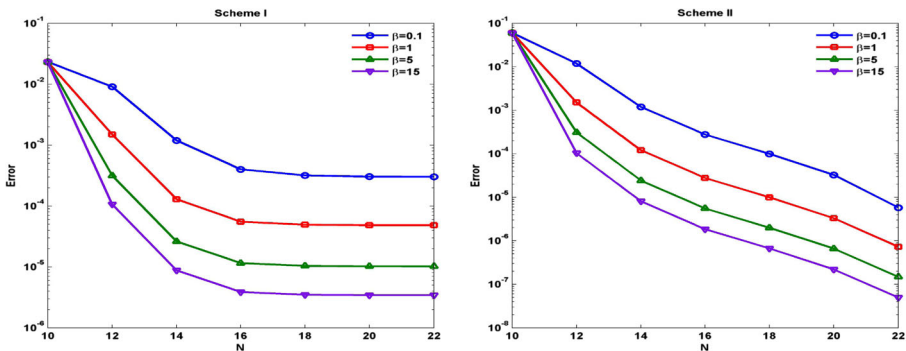


Fig. 2 l^2 -errors of Schemes I and II with $\tau = 0.001$ and different values of β and N for test problem 1

Table 6 Numerical results of proposed schemes in time variable for test problem 2 for $\alpha = 0.5$

τ	Scheme I			Scheme II		
	l^2 -error	CPU time	C-order	l^2 -error	CPU time	C-order
1/20	1.0061×10^{-3}	0.0065	–	3.8242×10^{-5}	0.0122	–
1/40	5.0945×10^{-4}	0.0139	0.9815	9.6214×10^{-6}	0.0198	1.9908
1/80	2.5633×10^{-4}	0.0216	0.9912	2.4129×10^{-6}	0.0373	1.9955
1/160	1.2856×10^{-4}	0.0468	0.9956	6.0418×10^{-7}	0.0826	1.9977
1/320	6.4383×10^{-5}	0.1229	0.9977	1.5117×10^{-7}	0.2089	1.9988
1/640	3.2217×10^{-5}	0.3555	0.9989	3.7806×10^{-8}	0.6067	1.9995
1/1280	1.6115×10^{-5}	1.2394	0.9994	9.4536×10^{-9}	2.0323	1.9997
1/2560	8.0589×10^{-6}	5.1819	0.9997	2.3637×10^{-9}	8.0000	1.9998
1/5120	4.0298×10^{-6}	24.583	0.9999	5.9097×10^{-10}	34.086	1.9999

Remark 6.1 For the exact solution of this test problem, we have $\frac{\partial^2 u(x,t)}{\partial t^2} = 0$, so from Lemma 2.1, we evaluate the fractional derivative exactly. Therefore, the order of schemes in time component depends to the order of approximating other terms in (1.1). Obviously, this order for Scheme I is 1 and for Scheme II is 2 and hence the computational orders reported in Tables 6 and 7 are compatible with theoretical ones.

Test problem 3:

As more realistic problem, we consider the following time fractional Burgers equation for $x \in [-2, 2]$

$${}_0 D_t^\alpha u(x, t) + u^p u_x - \beta u_{xx} = f(x, t). \tag{6.7}$$

with the so-called Maxwellian initial condition [22] which is a Gaussian pulse initially centered at $x = 0$ and is as follows

$$u(x, 0) = \exp(-bx^2). \tag{6.8}$$

Table 7 Computational order of proposed schemes in time variable for test problem 2 for $\alpha = 0.9$

τ	Scheme I			Scheme II		
	l^2 -error	CPU time	C-order	l^2 -error	CPU time	C-order
1/30	6.7655×10^{-4}	0.0072	–	1.7080×10^{-5}	0.0159	–
1/60	3.4111×10^{-4}	0.0168	0.9880	4.2880×10^{-6}	0.0281	1.9939
1/120	1.7127×10^{-4}	0.0335	0.9940	1.0743×10^{-6}	0.0602	1.9969
1/240	8.5813×10^{-5}	0.0795	0.9970	2.6885×10^{-7}	0.1395	1.9985
1/480	4.2951×10^{-5}	0.2261	0.9985	6.7251×10^{-8}	0.3822	1.9992
1/960	2.1487×10^{-5}	0.7310	0.9992	1.6819×10^{-8}	1.2155	1.9995
1/1920	1.0746×10^{-5}	2.6555	0.9997	4.2059×10^{-9}	4.1593	1.9996

Table 8 Numerical results of schemes I, II in time variable for Test problem 3 for $\alpha = 0.1$

τ	Scheme I		Scheme II	
	l^2 -error	C-order	l^2 -error	C-order
1/20	1.7516×10^{-2}	–	1.4304×10^{-3}	–
1/40	8.9035×10^{-3}	0.9762	3.6309×10^{-4}	1.9780
1/80	4.4870×10^{-3}	0.9886	9.1600×10^{-5}	1.9869
1/160	2.2521×10^{-3}	0.9944	2.3035×10^{-5}	1.9915
1/320	1.1282×10^{-3}	0.9972	5.7962×10^{-6}	1.9906
1/640	5.6466×10^{-4}	0.9986	1.4725×10^{-6}	1.9768
1/1280	2.8246×10^{-4}	0.9993	3.9332×10^{-7}	1.9045

For this problem

$$f(x, t) = \frac{2t^{2-\alpha}}{\Gamma(3-\alpha)} \exp(-bx^2) + (t^2 + 1)^{p+1} \exp(-2bx^2)(-2bx) - \beta(t^2 + 1)(-2b + 4b^2x^2) \exp(-2bx^2). \quad (6.9)$$

and the exact solution is $u(x, t) = (t^2 + 1) \exp(-bx^2)$. We set $T = p = \beta = 1$ and $b = 5$. Tables 8 and 9 present the results of Schemes I and II with $N = 32$, $\alpha = 0.2, 0.8$ and different values of τ .

Tables 8 and 9 show that the computational orders of scheme I, II in time component are approximately $\mathcal{O}(\tau)$ and $\mathcal{O}(\tau^{2-\alpha})$ respectively which are compatible with theoretical ones. Figure 3 shows the l^2 -error of Schemes I and II with $\alpha = 0.5$, $\tau = 0.001$ and different values of β and N which apparently the spatial spectral accuracy is verified.

Table 9 Numerical results of schemes I,II in time variable for test problem 3 for $\alpha = 0.7$

τ	Scheme I		Scheme II	
	l^2 -error	C-order	l^2 -error	C-order
1/20	1.5123×10^{-2}	–	3.3905×10^{-3}	–
1/40	7.7086×10^{-3}	0.9722	1.3322×10^{-3}	1.3476
1/80	3.8998×10^{-3}	0.9830	5.3502×10^{-4}	1.3161
1/160	1.9651×10^{-3}	0.9887	2.1662×10^{-4}	1.3044
1/320	9.8798×10^{-4}	0.9920	8.7943×10^{-5}	1.3005
1/640	4.9604×10^{-4}	0.9940	3.5741×10^{-5}	1.2990
1/1280	2.4882×10^{-4}	0.9954	1.4540×10^{-5}	1.2976
1/2560	1.2473×10^{-4}	0.9963	5.9276×10^{-6}	1.2945

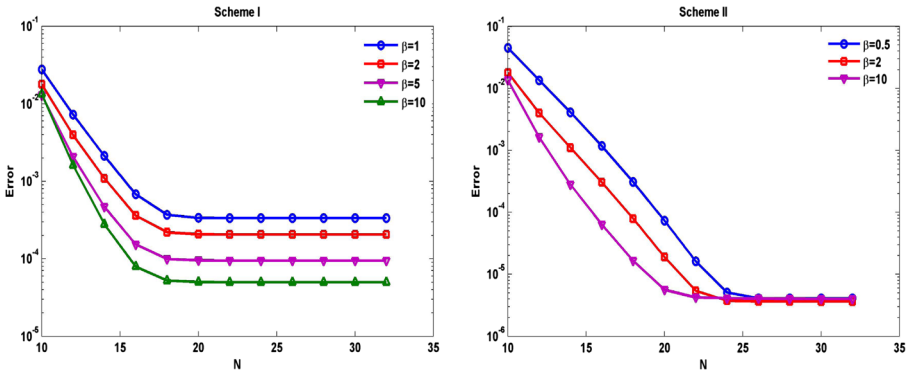


Fig. 3 l^2 -errors of Schemes I and II with $\tau = 0.001$ and different values of β and N for test problem 3

Test problem 4:

We examine the efficiency of proposed schemes for the solution of system of time fractional PDEs. To this end, we consider the following stochastic time fractional equation with additive noise

$${}^c D_t^\alpha u(x, t) + uu_x - u_{xx} + u_{xxx} + \sigma B(t) = 0, \quad x \in [-15, 15], \quad (6.10)$$

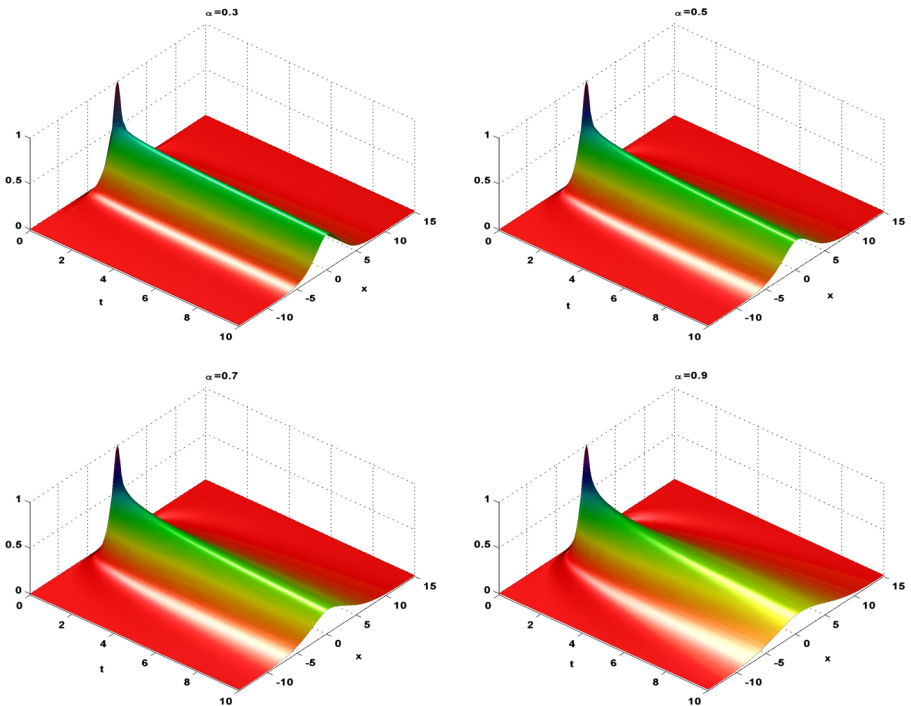


Fig. 4 Surface plots of approximate solution of test problem 4 with $\sigma = 0$ and different values of α

with initial condition

$$u(x, 0) = \text{sech}^2(x),$$

where the boundary conditions are periodic, σ is a constant that indicates the amplitude of noise and $B(t)$ is a Wiener process on $L^2(\mathbb{R})$ (the space of real valued square integrable functions on \mathbb{R}). We first solve deterministic version of problem ($\sigma = 0$). We put $T = 10$, $N = 128$, $\tau = 0.01$. Figure 4 presents the surface plots of approximate solution of this test problem for different values of α with Scheme II (plots of approximate solution using Scheme I are also similar to Scheme II).

Now, we investigate the effect of noise to the numerical solutions. After applying polynomial chaos (PC) expansion (see Appendix) to discretize the random variable, a coupled time fractional deterministic system of PDEs is obtained. For the resulting system of time fractional PDEs, we apply the the Scheme II. We put $N = 128$, $\tau = 0.01$, $K = 2$, $M = 3$ and $T = 1$. Figure 5 presents the mean of approximate solution of this problem for different values of α and σ . Figure 5 shows that for small values of α , for example $\alpha = 0.1$, we can get satisfactory results for the amplitude of σ up to $\sigma = 0.65$, while for large values of α , for example $\alpha = 0.8$, the solutions can be obtained even up to noise amplitude $\sigma = 9$. Figure 6 shows the pathwise solutions of this test problem for $\alpha = 0.5$ and $\sigma = 0.05, 0.25, 0.55, 0.7$.

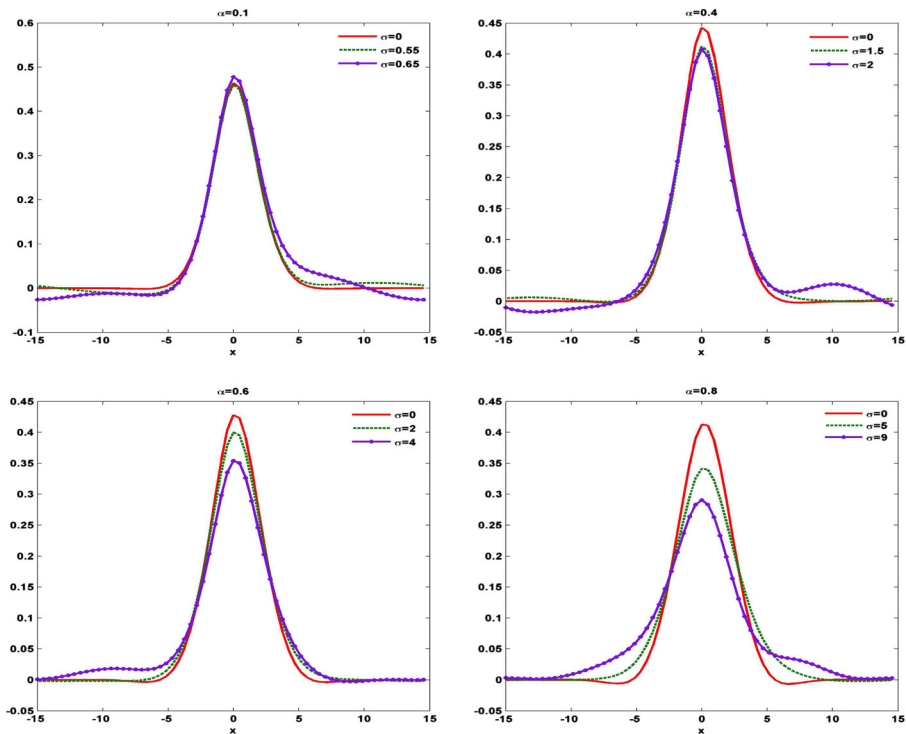


Fig. 5 Plots of the mean of approximate solution with different values of α and σ for test problem 4

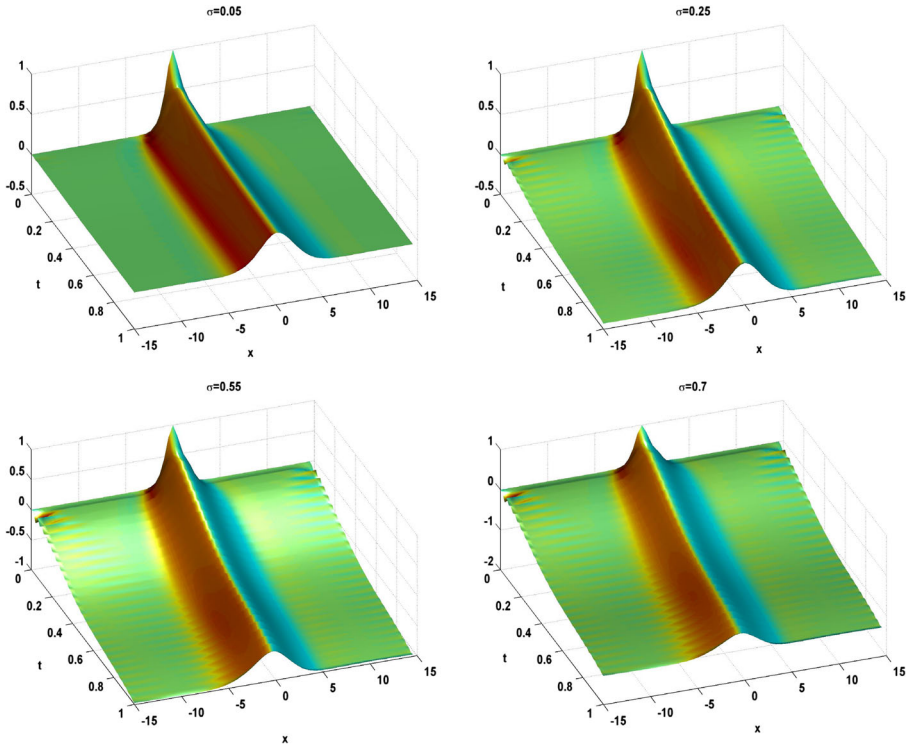


Fig. 6 Pathwise solutions of test problem 4 with $\alpha = 0.5$ and different values of σ

7 Conclusion

In this paper, we proposed two semi-implicit Fourier pseudospectral schemes for the solution of generalized time fractional Burgers type equations. We presented the consistency, stability, and convergence analysis of schemes, under some assumptions. During the computation, we used the fast Fourier transform (FFT). We compared our numerical results with analytical solutions and a recently reported result. We showed that the proposed schemes are more efficient in accuracy and computing time. Also, we have illustrated that the order of accuracy of the introduced schemes are in good agreement with the obtained theoretical ones. Finally, we reported the performance of the proposed schemes on solution of stochastic time fractional Burgers equation driven by Brownian motions.

Appendix

For fixed $T > 0$, we consider $e = \{e_i, i \geq 1\}$, as an orthonormal basis of $L_2([0, T])$, to be the trigonometric functions

$$e_1(t) = \frac{1}{\sqrt{T}}, \quad e_i(t) = \sqrt{\frac{2}{T}} \cos\left(\frac{(i - 1)\pi t}{T}\right), \quad i = 2, 3, \dots, \quad 0 \leq t \leq T.$$

Also define the independent standard Gaussian random variables $\xi_i = \int_0^T e_i(s)dB$.

Theorem A.1 ([28], Theorem 2.1) *The Brownian motion $\{B(t); 0 \leq t \leq T\}$ has the Fourier expansion*

$$B(t) = \sum_{i=1}^{\infty} \xi_i \int_0^t e_i(s)ds, \quad 0 \leq t \leq T, \tag{A.1}$$

which converges in the mean-square sense for all $t \leq T$, i.e.,

$$E \left(B(t) - \sum_{i=1}^n \xi_i \int_0^t e_i(s)ds \right)^2 \leq \frac{T}{\pi n},$$

where E is the expectation operator.

Now, consider the countable set of multi-indices

$$\mathfrak{J} = \{ \gamma = (\gamma_i), \quad i \geq 1, \quad \gamma_i \in \{0, 1, 2, \dots\} \},$$

with length $|\gamma| := \sum_i \gamma_i < \infty$. Define the collection $F = \{ \xi_\gamma, \gamma \in \mathfrak{J} \}$ of random variables such that

$$\xi_\gamma = \frac{1}{\sqrt{\gamma!}} \prod_i H_{\gamma_i}(\xi_i),$$

where $H_{\gamma_i}(\xi_i) = (-1)^{\gamma_i} e^{\frac{\xi_i^2}{2}} \frac{d^{\gamma_i}}{d\xi_i^{\gamma_i}} e^{-\frac{\xi_i^2}{2}}$ is the Hermite polynomial of order γ_i and $\gamma! = \prod_i \gamma_i!$. For more details about the above definition references, [21, 27] are useful.

Now, we can introduce polynomial chaos expansion method which separates the stochastic from the deterministic part of a random field. This expansion at first was introduced by Cameron and Martin [4] and generalized by Lototsky and Rozovsky in [27]. Suppose $\mathbb{W} = (\Omega, \mathcal{F}, P, \{ \mathcal{F}_t \}_{0 \leq t \leq T})$ be a probability space, where \mathcal{F}_t is the σ -algebra generated by the random variables $(\xi_i; i \in N)$ and denote by $L^2(\mathbb{W}; H)$ the separable Hilbert space of \mathcal{F}_T measurable square integrable H -valued random variables, where H is a Hilbert space.

Theorem A.2 ([21], Theorem 1) *If $u \in L^2(\mathbb{W}; H)$ and $u_\gamma = E[u\xi_\gamma] \in H$ then*

$$u = \sum_{\gamma \in \mathfrak{J}} u_\gamma \xi_\gamma. \tag{A.2}$$

More information about properties of polynomial chaos expansion method can be found in [38]. To make any use of (A.2) as a numerical scheme for the calculation of the solution, we need to truncate it into a finite sum. As is seen, the sum over $\gamma \in \mathfrak{J}$ is a doubly-infinite sum, so as a truncation of this multi-index set we consider the following finite set

$$\mathfrak{J}_f := \{ (\gamma_i) \in \mathfrak{J} : 1 \leq i \leq M, \quad |\gamma| \leq K \}.$$

The set \mathfrak{J}_f is finite with $\frac{(M+K)!}{M!K!}$ elements and the truncated solution of (A.2) is denoted by

$$u^f = \sum_{\gamma \in \mathfrak{J}_f} u_{\gamma}^f \xi_{\gamma}. \quad (\text{A.3})$$

References

1. Abdel-Salam, E.A.B., Hassan, G.F.: Multi-wave solutions of the space-time fractional Burgers and Sharma-Tasso-Olver equations. *Ain Shams Eng. J.* **7**, 463–472 (2016)
2. Abdel-Salam, E.A.B., Yousif, E.A., Arko, Y.A.S., Gumma, E.A.E.: Solution of moving boundary space-time fractional Burger's equation. *J. Appl. Math.* **2014**, Article ID 218092, 8 pages (2014)
3. Bhrawy, A.H., Zaky, M.A., Baleanu, D.: New numerical approximations for space-time fractional Burgers' equations via a Legendre spectral-collocation method. *Roman. Rep. Phys.* **67**, 340–349 (2015)
4. Cameron, R.H., Martin, W.T.: The orthogonal development of nonlinear functionals in series of Fourier-Hermite functionals. *Ann. Math.* **48**, 385–392 (1947)
5. Canuto, C., Quarteroni, A.: Approximation results for orthogonal polynomials in Sobolev spaces. *Math. Comput.* **38**, 67–86 (1982)
6. Cheng, K., Feng, W., Gottlieb, S., Wang, C.: A Fourier pseudospectral method for the “Good” Boussinesq equation with second-order temporal accuracy. *Numer. Methods Partial Differ. Eq.* **31**, 202–224 (2015)
7. Dehghan, M., Manafian, J., Saadatmandi, A.: Solving nonlinear fractional partial differential equations using the homotopy analysis method. *Numer. Methods Partial Differ. Eq.* **26**, 448–479 (2010)
8. Diethelm, K.: An algorithm for the numerical solution for differential equations of fractional order. *Elec. Trans. Numer. Anal.* **5**, 1–6 (1997)
9. W. E.: Convergence of Fourier methods for Navier-Stokes equations. *SIAM J. Numer. Anal.* **30**, 650–674 (1993)
10. El-Danaf, T.S., Hadhoud, A.R.: Parametric spline functions for the solution of the one time fractional Burgers' equation. *Appl. Math. Modell.* **36**, 4557–4564 (2012)
11. Esen, A., Tasbozan, O.: Numerical solution of time fractional Burgers equation by cubic B-spline finite elements. *Mediterr. J. Math.* **13**, 1325–1337 (2016)
12. Esen, A., Tasbozan, O.: Numerical solution of time fractional Burgers equation. *Acta Univ. Sapientiae, Mathematica* **7**, 167–185 (2015)
13. Esen, A., Bulut, F., Oru, O.: A unified approach for the numerical solution of time fractional Burgers type equations. *Eur. Phys. J. Plus* **131**, 116 (2016)
14. Gottlieb, S., Wang, C.: Stability and convergence analysis of fully discrete Fourier collocation spectral method for 3-D viscous Burgers equation. *J. Sci. Comput.* **53**, 102–128 (2012)
15. Guo, B.Y., Zou, J.: Fourier spectral projection method and nonlinear convergence analysis for Navier-Stokes equations. *J. Math. Anal Appl.* **282**, 766–791 (2003)
16. Guo-Cheng, W.: Lie Group Classifications and Non-differentiable Solutions for Time-Fractional Burgers Equation. *Commun. Theor. Phys.* **55**, 1073–1076 (2011)
17. Gupta, A.K., Saha Ray, S.: On the solutions of fractional Burgers-Fisher and generalized Fisher's equations using two reliable methods. *Int. J. Math. Math. Sci.* **2014**, Article ID 682910, 16 pages (2014)
18. Inc, M.: The approximate and exact solutions of the space- and time-fractional burgers equation with initial conditions by variational iteration method. *J. Math. Anal. Appl.* **345**, 476–484 (2008)
19. Jin, B., Lazarov, R., Zhou, Z.: An analysis of the L1 scheme for the subdiffusion equation with nonsmooth data. *IMA J. Numer. Anal.* **36**, 197–221 (2016)
20. Jin, B., Zhou, Z.: An analysis of the Galerkin proper orthogonal decomposition for subdiffusion. *ESAIM: Math. Modeling Numer. Anal.* (in press). arXiv:1508.06134
21. Kalpinielli, E.A., Frangos, N.E., Yannacopoulos, A.N.: Numerical methods for hyperbolic SPDEs: a Wiener chaos approach. *Stoch PDE Anal. Comp.* **4**, 606–633 (2013)

22. Kang, X., Cheng, K., Guo, C.: A second-order Fourier pseudospectral method for the generalized regularized long wave equation. *Adv. Diff. Eq.* **2015**, 339 (2015)
23. Khan, N.A., Ara, A., Mahmood, A.: Numerical solutions of time-fractional Burger equations: a comparison between generalized transformation technique with homotopy perturbation method. *Int. J. Num. Method Heat Fluid Flow* **22**, 175–93 (2012)
24. Lakestani, M., Dehghan, M.: Numerical solutions of the generalized Kuramoto-Sivashinsky equation using B-spline functions. *Appl. Math. Modell.* **36**, 605–617 (2012)
25. Li, D., Zhang, C., Ran, M.: A linear finite difference scheme for generalized time fractional Burgers equation. *Appl. Math. Modell.* **40**, 6069–6081 (2016)
26. Lin, Y., Xu, C.: Finite difference/spectral approximations for the time-fractional diffusion equation. *J. Comput. Phys.* **225**, 1533–1552 (2007)
27. Lototsky, S., Rozovsky, B.: Stochastic differential equations: a Wiener chaos approach. In: Kabanov, Y., Liptser, R., Stoyanov, J. (eds.) *From Stochastic Calculus to Mathematical Finance: The Shiryaev Festschrift*, pp. 433–507. Springer, Berlin (2006)
28. Lue, W.: Wiener chaos expansion and numerical solutions of stochastic partial differential equations. PhD Thesis, California Institute of Technology, Pasadena (2006)
29. Mohebbi, A., Abbaszadeh, M.: Compact finite difference scheme for the solution of time fractional advection-dispersion equation. *Numer. Algor.* **63**, 431–452 (2013)
30. Quarteroni, A., Valli, A.: Numerical approximation of partial differential equations. *Springer Series in Computational Mathematics*, vol. 23. Springer-Verlag (1994)
31. Tadmor, E.: Convergence of spectral methods to nonlinear conservation laws. *SIAM J. Numer. Anal.* **26**, 30–44 (1989)
32. Tadmor, E.: The exponential accuracy of Fourier and Chebyshev differencing methods. *SIAM J. Numer. Anal.* **23**, 1–10 (1986)
33. Sahoo, S., SahaRay, S.: New approach to find exact solutions of time-fractional Kuramoto-Sivashinsky equation. *Physica A* **434**, 240–245 (2015)
34. Song, L., Zhang, H.Q.: Application of homotopy analysis method to fractional KDV-Burgers-Kuramoto equation. *Phys. Lett. A.* **367**, 88–94 (2007)
35. Sugimoto, N.: Burgers equation with a fractional derivative; hereditary effects on nonlinear acoustic waves. *J. Fluid Mech.* **225**, 631–653 (1991)
36. Sugimoto, N.: Generalized Burgers equation and fractional calculus. In: *Nonlinear wave motion*. Longman Scientific and Technical (1989)
37. Sun, Z.Z., Wu, X.: A fully discrete difference scheme for a diffusion-wave system. *Appl. Numer. Math.* **56**, 193–209 (2006)
38. Xiu, D., Karniadakis, G.E.: The Wiener-Askey polynomial chaos for stochastic differential equations. *SIAM J. Sci. Comput.* **24**, 619–644 (2002)
39. Wang, Q.: Numerical solutions for fractional kdv-burgers equation by adomian decomposition method. *Appl. Math. Comput.* **182**(2), 1048–1055 (2006)